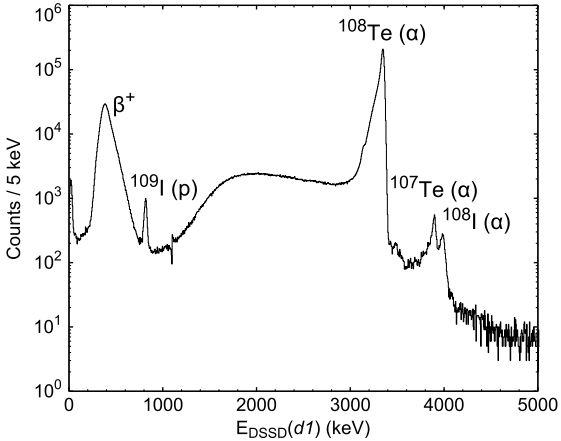


**Fig. 2.** Energy spectrum for all decay events observed as a member of a *R-d1* event chain. The previously known activities are labeled. The discontinuity at the energy of 1100 keV is due to the different energy calibration for proton- and $\alpha$-decay events.

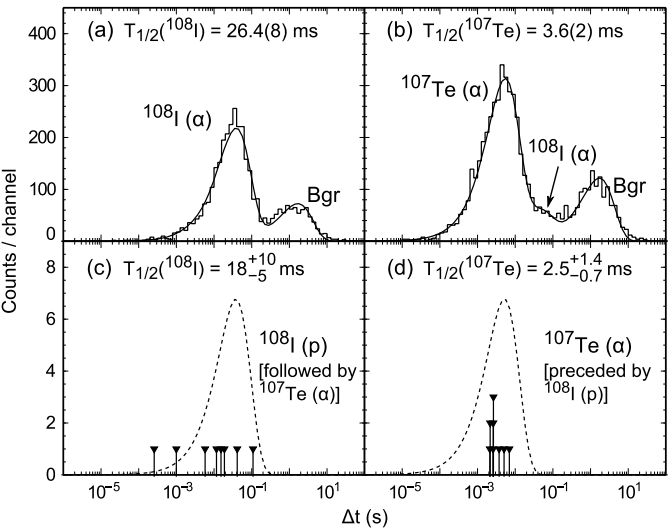


**Fig. 3.** Time difference between a recoil implantation and a subsequent decay event observed in the same pixel of the DSSD, when the decay is (a) $^{108}$I($\alpha$), (b) $^{107}$Te($\alpha$) or (c) $^{108}$I($p$) followed by the $\alpha$ decay of $^{107}$Te. In panel (d), the time difference between two subsequent decay events of $^{108}$I($p$) and $^{107}$Te($\alpha$) is presented. The quoted half-lives were obtained with the logarithmic time-scale method [35] (panels (a) and (b)) or maximum likelihood method [36] (panels (c) and (d)). The solid lines in (a) and (b) are fits to the data, and the dashed lines in (c) and (d) are the probability density distributions [35] corresponding to the half-lives obtained from these fits. The peak labeled "Bgr" corresponds to random correlations, see text for details.

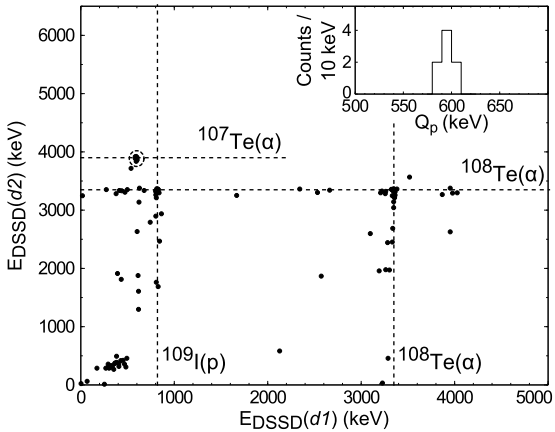


**Fig. 4.** Energy-energy correlation matrix for two subsequent decay events in *R-d1-d2* chains, when the *R-d1* and *d1-d2* time differences are less than 130 ms and 18 ms, respectively. The inset provides the energy spectrum of the newly observed $^{108}$I proton decay events, which are highlighted with a dashed circle in the main panel. Due to a high count rate in the DSSD and the long half-life, $^{108}$Te $\alpha$-decay events self-correlate randomly. The dashed lines mark the energies of selected, previously identified, charged-particle decay activities in this region.

**Table 1**
$Q$ values, half-lives $T_{1/2}$, and mass excesses $\Delta$ obtained in the present study compared to the literature values.

| Quantity | This work | AME2016 [31,38,39] | Other studies | |
|---|---|---|---|---|
| $Q_p(^{108}\mathrm{I})$ (keV) | 597(13) | 600(110) | ≥240 | [19] |
| | | | ≲600 | [26] |
| $Q_p(^{104}\mathrm{Sb})$ (keV) | 510(20) | 510(100) | ≥150 | [19] |
| | | | ≤520 | [19] |
| | | | ≲550 | [26] |
| $Q_\alpha(^{108}\mathrm{I})$ (keV) | 4097(10) | 4100(50) | 4099(5) | [26] |
| $Q_\alpha(^{107}\mathrm{Te})$ (keV) | 4007(10) | 4008(5) | 3982(16) | [40] |
| | | | 4012(10) | [32] |
| $Q_\alpha(^{112}\mathrm{Cs})$ (keV) | 3940(20) | 3930(120) | ≥3830 | [19] |
| | | | ≤4210 | [19] |
| | | | ≲3940 | [29] |
| $T_{1/2}(^{107}\mathrm{Te})$ (ms) | 3.6(2) | 3.1(1) | $3.6^{+0.6}_{-0.4}$ | [40] |
| | | | 3.1(1) | [29] |
| $T_{1/2}(^{108}\mathrm{I})$ (ms) | 26.4(8) | 36(6) | 36(6) | [29] |
| $\Delta(^{104}\mathrm{Sb})$ (MeV) | -59.17(8) | -59.17(12) | | |
| $\Delta(^{108}\mathrm{I})$ (MeV) | -52.65(8) | -52.65(13) | | |